

# Hall Probe Magnetic Measurements of a Superconducting Undulator

V. M. Tsukanov<sup>a, b, \*</sup>, S. V. Khrushchev<sup>a, b</sup>, A. A. Volkov<sup>a, b</sup>, A. V. Zorin<sup>a</sup>, P. V. Kanonik<sup>a</sup>,  
N. A. Mezentsev<sup>a, b</sup>, and V. A. Shkaruba<sup>a, b</sup>

<sup>a</sup> Budker Institute of Nuclear Physics, Siberian Branch, Russian Academy of Sciences, Novosibirsk, 630090 Russia

<sup>b</sup> Synchrotron Radiation Facility, Siberian Circular Photon Source, Boreskov Institute of Catalysis,  
Siberian Branch, Russian Academy of Sciences, Koltsovo, 630559 Russia

\*e-mail: tsukanov@inp.nsk.su

Received November 28, 2022; revised December 15, 2022; accepted January 25, 2023

**Abstract**—The superconducting undulator with a 15.6-mm period and a 1.2-T magnetic field, described in this article, has a 8-mm magnetic gap. The magnetic measuring system under such conditions requires the use of a special tube (ante-chamber) inside the undulator’s magnetic gap. The thermal insulation between the cold magnet and this measuring tube is not enough to have a stable temperature along full length of the tube. The range of temperatures in this tube is 55–300 K. Hall probe measurements in this case are a complicated problem. Ways of measuring and processing results are described.

DOI: 10.3103/S1062873822701854

## INTRODUCTION

Most of the insertion devices now manufactured by BINP have a cryogenic system based on indirect cooling. The magnetic system is not in liquid helium, but in a vacuum. This allows us to reduce the inter-pole gap and increase the working field of the undulator. The aperture of the undulator’s vacuum chamber is 6 mm. This is not enough to install a measuring chamber and conduct magnetic measurements, so a measuring chamber is installed instead of a vacuum chamber during tests.

## MEASURING CHAMBER

Our measuring chamber was manufactured using a standard profile made of AD-31 alloy (a rectangular extruded thin-walled pipe with an internal cross section of  $21 \times 5$  mm, produced by Sibprofil Novosibirsk). The inner surface of the measuring chamber is in contact with the atmosphere, while the outer one is separated from the magnetic system with a temperature below 4 K by a vacuum gap. To reduce the flow of heat from the chamber to the magnet and for thermal insulation of the measuring volume, the chamber was covered with several layers of special cryogenic super insulation, on top of which a copper foil screen 0.2 mm thick was installed (Fig. 1). A 0.2 mm nylon fishing line was wound over the copper screen with a large pitch to prevent direct contact between it and the magnet.

Despite such measures, it is impossible to ensure good thermal insulation with such narrow gaps. The temperature of the measuring carriage therefore varies

in the range of 300 to 55 K when moving along the chamber. The temperatures of phase transitions of the main atmospheric gases are in this range (Table 1). These gases can be inside the measuring chamber in all their states. Two effects were observed during tests. When returning after the end of the scan, the carriage worked like a piston, which sometimes resulted in intense outpouring of liquid gas from the chamber. A negligible amount of snow (most likely carbon diox-

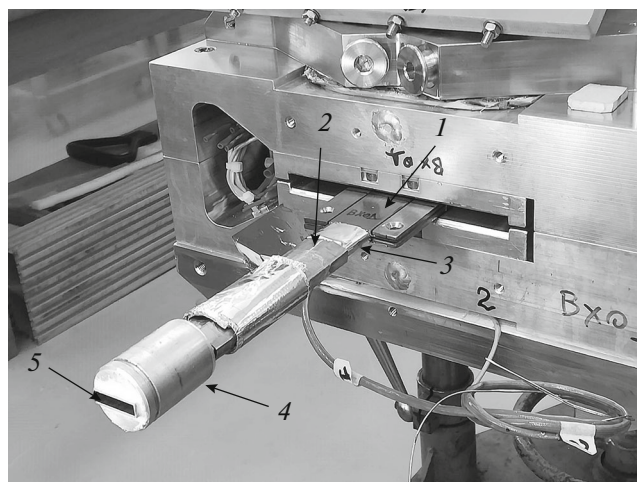


**Fig. 1.** Measuring chamber inside the undulator’s magnetic system. (1) Copper screen of the measuring chamber, (2) multilayer magnetic screen, (3) measuring chamber thermal insulation, (4) cylindrical sliding assembly, and (5) measuring chamber.

**Table 1.** Temperatures of phase transitions of the main atmospheric gases.

Gas	Temperature of condensation, K	Temperature of crystallization, K
Nitrogen	77	63
Oxygen	90	54
Carbon dioxide	—	194.5

ide, which does not have a liquid phase) was also observed when purging the measuring chamber with compressed helium.

The measuring chamber is installed into the flanges at its ends with the ability to move vertically. This allows us to compensate for the displacement of the magnet during cooling.

The temperature of the chamber changes considerably as the undulator operates, altering the length of the former. To compensate for this effect, sliding cylindrical sealing units are glued to the ends of the chamber.

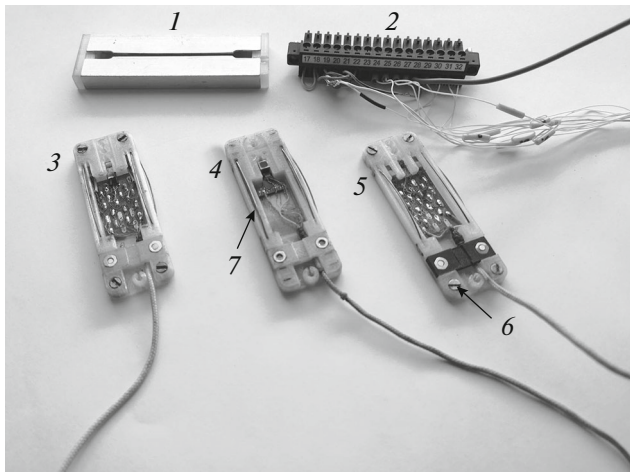


**Fig. 2.** Measuring carriages of different configurations. (1) Pencil case for storing and calibrating carriages, (2) socket for connecting to the NI-6218 ADC, (3) carriage with three HE244 probes for measuring the main and horizontal fields with the possibility of shifting the carriage vertically, (4) carriage with a 3-D HE444 probe, (5) carriage with three horizontally positioned HGT1050 probes, (6) mounting screws for changing the position relative to the median, and (7) pressure springs for fixing the carriage relative to the measuring chamber. The mounting screws provide a vertical offset of  $\pm 0.4$  mm from the chamber's center.

Multilayer magnetic screens are installed at the beginning and end of the chamber to create zero-field sections (Fig. 1).

## UNDULATOR MAGNETIC SYSTEM

The undulator's magnetic system has a design very different from the ones commonly used [1–3]. There are poles of only one polarity on each half of the magnet, and they alternate with neutral poles.

In this configuration, the winding end sections form two long longitudinal coils with counter-propagating fields. This produces the skew quadrupole components of the magnetic field. To compensate for this effect, the ratio of the lengths of the coil cores and neutral poles are calculated so as to ensure maximum suppression of parasitic components on the beam's trajectory in the operating mode. For more accurate correction and expansion of the undulator's operating range, long superconducting corrective windings are included in its design.

Uncompensated fields of the first and last windings are also a feature of this magnetic system's design. This produces a large longitudinal component of the magnetic field at the ends of the system. Longitudinal correctors are used to reduce this effect.

Strict requirements for the phase error are imposed on the undulator. The undulator's design allows prompt correction of the field. The magnetic system is evenly divided into 24 groups with 12 coils on each half, and the current leads are distributed to supply power to each group independently. If necessary, additional currents are supplied from additional power sources to selected corrected groups according to a preliminarily calculated table.

## EQUIPMENT

The undulator's design place additional requirements on magnetic measurements. We currently use several types of measuring carriages, all of which are made of polycarbonate using 3D modeling and printing technology. Using a 3D printer allows us to quickly develop and manufacture carriages with any option for installing Hall probes (Fig. 2).

Probes from two manufacturers (Hoeben Electronics (HE244 and HE444) with an operating current of 1 mA and LakeShore (HGT1050) with an operating current of 100 mA) are used for measuring. Thermistors are installed in all carriages to measure the temperature of the probes during scanning. It is convenient to use the operating current of Hall probes for measuring temperature. At a current of 1 mA, it is best to use standard Pt100 (100 ohms) miniature platinum thermistors. A thermistor with a resistance of no more than 1 Ohm is required for a current of 100 mA. We could find nothing suitable, so we decided to produce

one of our own. We manufactured miniature frameless coils wound with a folded copper wire 0.07 mm in diameter and having a resistance of around 0.5 ohms. Since the calibration of Hall probes is tied not to temperature but to the voltage on a temperature probe installed in the carriage, the accuracy of measuring temperature does not matter.

Compact test magnets with fields of 0.9 and 0.7 T were manufactured for the preliminary evaluation and selection of probes.

Two carriages with the possibility of shifting the scanning trajectory vertically by  $\pm 0.4$  mm were designed and manufactured to estimate the vertical structure of the magnetic field. First carriage had three HGT1050 probes arranged horizontally; the second one contained three HE244 probes, the middle one of which was positioned horizontally. The two outermost probes were arranged vertically with a space of 14 mm between them to measure the horizontal component of the field.

#### TEMPERATURE CORRECTION OF HALL PROBE MEASUREMENTS

The Hall probe parameters had an individual temperature dependence for each probe. It is therefore desirable to stabilize the temperature of the probe or provide temperature correction of the measurements in order to obtain good results. It is almost impossible to stabilize the temperatures of the probes in such a wide range of temperatures and such size. We therefore decided to calibrate the Hall probes in a wide range of temperatures. The carriages with Hall probes thus contained temperature probes that recorded the real temperature at the moment of measuring. The evaporation of liquid nitrogen was used to alter the temperature over a wide range of values.

Calibration was done in two stages. At the first stage, we obtained the dependence of zero voltage of the Hall probes on temperature. This work presents results from calibrating a carriage with three HGT1050 probes.

To calibrate zero, the carriage was placed in a magnetic screen and filled with nitrogen. The resulting dependence of zero voltage on temperature was used in processing our measuring results.

A calibration magnet with an NMR meter and a maximum field of up to 2 T was used for calibrating in a magnetic field. Calibration was done in a field of 1.4 T, which was close to the undulator's operational field.

A standard Lake Shore 120 current source was used in calibration and measurements, with the possibility of setting the current stepwise in the range of 30  $\mu$ A–300 mA.

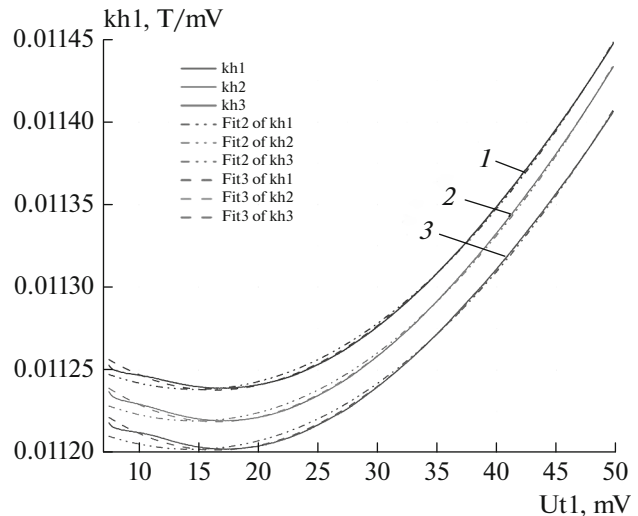


Fig. 3. The dependence of the Hall coefficients on the temperature varying from the liquid nitrogen to room ones for the HGT1050\*3 carriage and the results of fitting with polynomials of the (dash-dotted line) second and (dashed line) third orders.

Two complete temperature cycles in fields of different polarities were used in calibration. Results were processed with second- and third-order polynomials that were also used to process measuring results. The difference between the polynomials was negligible, but was obviously preferable to use a third-order polynomial (Fig. 3).

The ratios of the Hall coefficients in fields of different polarity differed considerably for different probes. It was also noticed that this parameter was virtually independent of temperature, so there was no need to make additional measurements of the Hall coefficient in the field of the second polarity throughout the range of temperatures (which would be quite laborious and bad for the probes). Below, the temperature calibration of the carriage was made in a field of one polarity, and the ratio of the coefficients was determined using a test magnet at room temperature.

Figure 4 shows the effect of temperature calibration on the results from processing our data in a field of 1.15 T. The main contribution to the measuring error was made by the dependence of the zero voltage on temperature, and that of the Hall coefficient on the polarity of the field.

#### MEASURING RESULTS

The main task we face in the current test of the undulator is minimizing the phase error and correction of errors caused by the vertical asymmetry of the undulator poles. Correcting the phase error requires several consecutive iterations. The measured magnetic

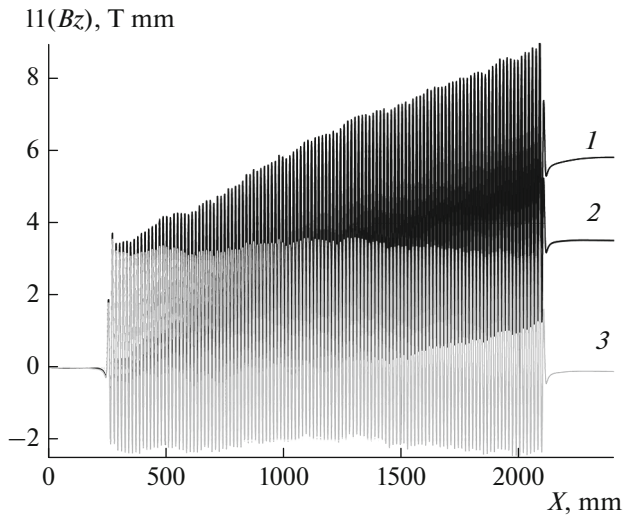


**Fig. 4.** The result of the influence of temperature corrections on the first integral of the undulator field. (1) Without considering temperature corrections, (2) temperature correction of zero, correction of zero and  $kh+$ , and correction of zero and  $kh-$ , and (3) considering the dependence of the Hall coefficient on the field polarity. The main contribution to the result is made by the temperature correction of zero and considering the dependence of the Hall coefficient on the field polarity.

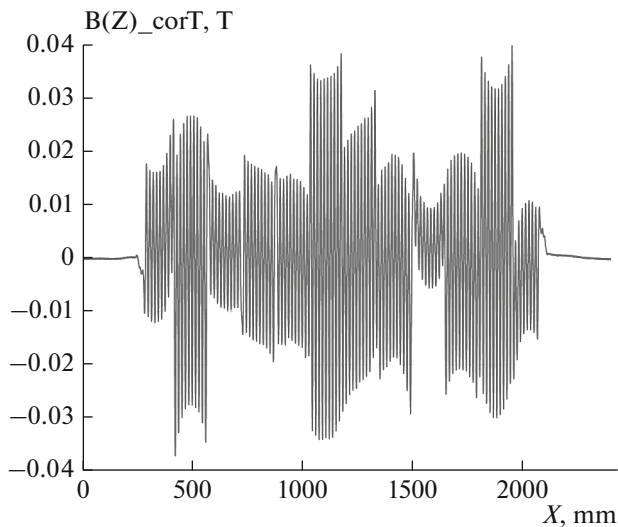


**Fig. 5.** Example of a phase error correction field.

field is analyzed and a table of correcting currents is generated with a specially written program. Correcting currents from additional sources are fed to groups of coils of the undulator, and the next measurement of the field is made. The graphs show an example of a correcting field (Fig. 5) and the result the correction effect had on the second integral (Fig. 6).

Longitudinal and transverse fields were also measured during the tests. This was done with the Hall 3D

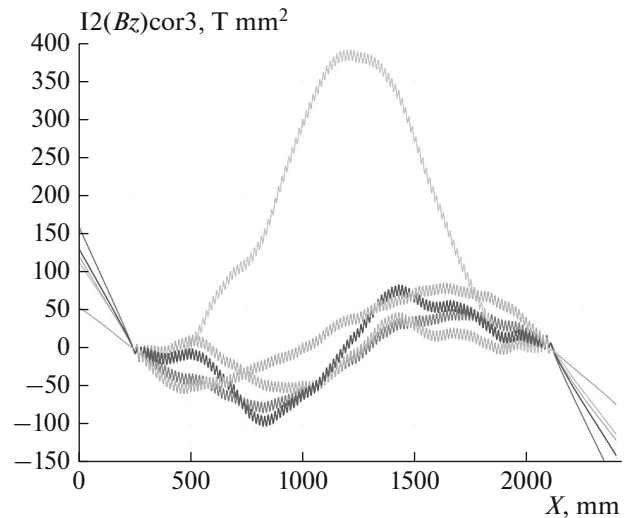


**Fig. 6.** Effect of the correcting field on the trajectory of the beam.

probes (HE 444) we have been using since 2015 (CLIC 2015, Delta 2018, KISI 2019) [4–8]. After assembly and cooling, there is always the question of the current position of the magnetic system. Measuring the longitudinal field allows us to determine the position of the measuring plane relative to the magnetic system's true median. The longitudinal field in the median plane should be minimal in wigglers with designs symmetrical around the median.

Design features of the undulator's magnetic system require a more thorough study of the magnetic field's structure. Despite the smallness of the measuring chamber, we manufactured measuring carriages with the possibility of vertically displacing the trajectory of scanning. Measurements with different vertical displacement were made to determine the actual position of a measuring chamber. The minimum magnetic field is the criterion for determining the median position of the magnetic system, relative to the center of the measuring chamber. Measurements showed that the measuring chamber fell by 0.2 mm during the cooling process.

## CONCLUSIONS

Work with the undulator prototype continues. Not all questions have been answered. The use of 3D printing in testing allowed us to quickly develop and manufacture measuring carriages of any configuration. The development and manufacture of plastic products (full cycle) can take about 1 day.



## FUNDING

This work was performed as part of Agreement no. 075-15-2021-1359 with the RF Ministry of Science and Higher Education, and State Task no. FWUS-2021-0004 for the Institute of Solid State Chemistry and Mechanochemistry.

## CONFLICT OF INTEREST

The authors declare that they have no conflicts of interest.

## REFERENCES

1. Khrushchev, S., Kanonik, P., Lev, V., et al., *AIP Conf. Proc.*, 2020, vol. 2299, p. 020012.
2. Mezentsev, N.A., Khrushchev, S.V., Shkaruba, V.A., et al., *Proc. 25th Russian Particle Accelerator Conf.*, St. Petersburg, 2016, p. TUCAMH01.
3. Khrushchev, S., Mezentsev, N., Shkaruba, V., et al., *Phys. Procedia*, 2016, vol. 84, p. 62.
4. Bragin, A., Bernhard, A., Casalbuoni, S., et al., *IEEE Trans. Appl. Supercond.*, 2016, vol. 26, no. 4, p. 4102504.
5. Bragin, A., Gusev, Ye., Khrushchev, S., et al., *Phys. Procedia*, 2016, vol. 84, p. 54.
6. Mezentsev, N., Bragin, A., Khrushchev, S., et al., *Proc. Russian Particle Accelerator Conf. RuPAC2018*, Protvino, 2018, p. 410.
7. Valentinov, A., Korchuganov, V., Ushakov, V., et al., *Proc. Russian Particle Accelerator Conf. RuPAC2018*, Protvino, 2018, p. 407.
8. Shkaruba, V., Bragin, A., Erokhin, A., et al., *AIP Conf. Proc.*, 2020, vol. 2299, p. 020005.

*Translated by N. Petrov*